



University of Warwick institutional repository: <http://go.warwick.ac.uk/wrap>

This paper is made available online in accordance with publisher policies. Please scroll down to view the document itself. Please refer to the repository record for this item and our policy information available from the repository home page for further information.

To see the final version of this paper please visit the publisher's website. Access to the published version may require a subscription.

Author(s): Stewart Ranson

Article Title: Longer-range distances by spinning-angle-encoding solid-state NMR spectroscopy

Year of publication: 2011

Link to published article:

<http://dx.doi.org/10.1039/C0CP02364G>

Publisher statement: None

# Longer-range distances by spinning-angle-encoding solid-state NMR spectroscopy

Johanna Becker-Baldus,<sup>a,b</sup> Thomas F. Kemp,<sup>a</sup> Jaan Past,<sup>c</sup> Andres Reinhold,<sup>c</sup> Ago Samoson<sup>\*a,c</sup> and Steven P. Brown<sup>\*a</sup>

<sup>5</sup> Received (in XXX, XXX) Xth XXXXXXXXX 200X, Accepted Xth XXXXXXXXX 200X

First published on the web Xth XXXXXXXXX 200X

DOI: 10.1039/b000000x

A new spinning-angle-encoding spin-echo solid-state NMR approach is used to accurately determine the dipolar coupling corresponding to a C-C distance over 4 Å in a fully labelled dipeptide. The dipolar coupling  
10 dependent spin-echo modulation was recorded off magic angle, switching back to the magic angle for the acquisition of the free-induction decay, so as to obtain optimum sensitivity. The retention of both ideal resolution and long-range distance sensitivity was achieved by redesigning a 600 MHz HX MAS NMR probe to provide fast angle switching during the NMR experiment: For 1.8 mm rotors, angle changes of up to ~5 degrees in ~10 ms were achieved at 12 kHz MAS. A new experimental design that combines a reference and a  
15 dipolar-modulated experiment and a master-curve approach to data interpretation is presented.

## Introduction

Applications of solid-state NMR encompassing biological solids, pharmaceuticals, supramolecular self-assembly and materials science exploit dipolar couplings to measure  
20 distances.<sup>1-2</sup> In particular, protocols for the determination of three-dimensional structures of biomacromolecules rely upon establishing multiple distance constraints via the inherent inverse cubed dependence on the internuclear distance of a  
25 dipolar coupling between two nuclear spins. While utilising dipolar couplings between nuclei with a short through-bond connectivity in the same or neighbouring amino acid residues is important for the assignment of the resonances, it is longer-range distances (> 4 Å) corresponding to inter-residue  
30 proximities between nuclei with no through-bond connectivity that are key to determining the secondary and tertiary structure of a protein.<sup>3-7</sup>

For isolated spin pairs in selectively labelled molecules, homonuclear dipolar couplings can be accurately determined,  
35 e.g., by double-quantum magic-angle spinning (MAS) <sup>13</sup>C build-up.<sup>8</sup> By comparison, distance measurements in multi-spin systems are challenging. Notably, "dipolar truncation", i.e., the dominant effect of the much larger one bond C-C  
40 dipolar couplings<sup>9-12</sup> hinders the measuring of the key longer-range distances (> 4 Å) in fully <sup>13</sup>C-labelled biomacromolecules. Indeed, developing new solid-state NMR approaches to overcome this problem is a current research priority for a number of groups worldwide. Advanced recoupling pulse sequences that seek to counteract dipolar  
45 truncation have been presented,<sup>13-18</sup> while rotational resonance (R<sup>2</sup>) experiments, i.e., fitting magnetization exchange at a R<sup>2</sup> condition<sup>19-20</sup> and modifications, e.g., the R<sup>2</sup> in the tilted frame (R<sup>2</sup>TR)<sup>21</sup> and R<sup>2</sup> width (R<sup>2</sup>W)<sup>22-23</sup> methods enable  
50 longer distances to be accurately measured, although typically only for nuclei with large chemical shift differences.

In a simple recently presented method, scaled residual dipolar couplings are detected in spin-echo experiments recorded off the magic angle.<sup>24-25</sup> Specifically, in an approach analogous to that used in selective REDOR and *J* spin-echo  
55 experiments,<sup>26-28</sup> the selective probing of the dipolar coupling between a specific pair of <sup>13</sup>C nuclei is achieved by a double-Gaussian spin-echo inversion pulse.<sup>25</sup> However, in this previously presented fixed angle experiment, the chosen spinning angle is a compromise that optimises neither dipolar  
60 modulation nor resolution. Moreover, it has to date only been shown that distances up to 2.2 Å corresponding to one- and two-bond connectivities could be determined by the off-MAS spin-echo method.<sup>25</sup>

By using a new switched-angle spinning probe design, this  
65 paper presents an uncompromised technical approach to the implementation of the off-MAS spin-echo method that retains both ideal resolution and long-range distance sensitivity. Specifically, a new protocol that combines a reference and a dipolar-modulated experiment as well as a master-curve for  
70 data interpretation is shown to allow the dipolar coupling corresponding to an effective C-C distance over 4 Å to be accurately determined in a fully labeled dipeptide.

## Experimental details

U-<sup>13</sup>C, <sup>15</sup>N *L*-histidine.HCl.H<sub>2</sub>O and 1-<sup>13</sup>C *L*-alanine were  
75 obtained from Cambridge Isotope Laboratory (Andover, MA, USA) and used without further purification. The Ac-VL dipeptide was synthesized by Peptide Synthesis Ltd (Fareham, UK) using U-<sup>13</sup>C, <sup>15</sup>N *L*-valine and U-<sup>13</sup>C, <sup>15</sup>N *L*-leucine as supplied by Cambridge Isotope Laboratory (Andover, MA,  
80 USA). The sample was re-crystallized from a 1:1 mixture of water and acetone, with crystals formed by slow evaporation of the solvent.<sup>29</sup>

The pulse sequence employed is depicted in Fig. 1, with the dipolar coupling dependent spin-echo modulation being

recorded off magic angle, switching back to the magic angle for acquisition, to optimise sensitivity. A 600 MHz HX 1.8 mm MAS NMR probe was redesigned to provide fast angle switching *during* the NMR experiment: angle changes of up to ~5 degrees in ~10 ms were achieved at 12 kHz MAS. Details of the angle-switching mechanism are given in the ESI.

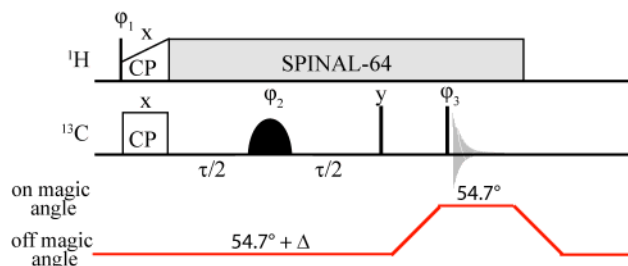


**Fig. 1** Switched-angle off-MAS spin-echo pulse sequence, employing SPINAL-64  $^1\text{H}$  decoupling<sup>30</sup> and a double-Gaussian inversion pulse to selectively probe the dipolar coupling due to a specific pair of  $^{13}\text{C}$  nuclei.

Experiments were performed on a Bruker Avance II+ spectrometer operating at  $^1\text{H}$  and  $^{13}\text{C}$  Larmor frequencies of 599.4 and 150.7 MHz, respectively, using a 1.8 mm double-resonance probe at a rotation frequency of 12 kHz. The  $^1\text{H}$  and  $^{13}\text{C}$   $90^\circ$  pulse lengths were 2.5 and 3.0  $\mu\text{s}$ , respectively. SPINAL-64  $^1\text{H}$  decoupling<sup>30</sup> at 100 kHz was used during the spin-echo period,  $\tau$ , the  $z$ -filter and acquisition. A 1 ms contact time was used for cross polarization from  $^1\text{H}$  to  $^{13}\text{C}$  with a 70 to 100 % ramp on the  $^1\text{H}$  channel.<sup>31-32</sup> The recycle delay was 3 s. For each spin-echo duration,  $\tau$ , 16 transients were co-added. A 16 step phase cycle was used:  $\phi_1 = y, -y$ ;  $\phi_2 = x, x, y, y$ ;  $\phi_3 = x, x, x, x, y, y, y, y, -x, -x, -x, -x, -y, -y, -y, -y$ ;  $\phi_{\text{rec}} = x, -x, -x, x, y, -y, -y, y, -x, x, x, -x, -y, y, y, -y$  (the pulse phases are indicated in Fig. 1).

As for previous (on-angle) MAS spin-echo experiments for determining  $J$  couplings,<sup>33-36</sup> the spin-echo intensity,  $s(\tau)$ , is obtained by integration over the corresponding lineshape (after Fourier transformation with respect to the acquisition time,  $t_2$ ). As discussed further in the ESI, this ensures that only in-phase lineshapes with their cosine spin-echo modulation are considered, i.e., there is no contribution from anti-phase lineshapes which have a sine spin-echo modulation.  $^1\text{H}$  decoupling is kept on during the  $z$ -filter delay in order to suppress spin diffusion that would otherwise affect an unwanted transfer of magnetisation between the spins. Error bars on fitted parameters are determined by the covariance method, as described in Ref.<sup>35</sup>

## Results and discussion

Fig. 2a and 2b present integrated off-MAS  $^{13}\text{C}$  spin-echo  $(\tau/2 - \pi - \tau/2)$  intensities,  $s(\tau)$ , obtained using the pulse sequence in Fig. 1 for a representative range of distances: CO-C $\beta$ , CO-C $\delta$ , CO-C $\epsilon$  in U- $^{13}\text{C}$ ,  $^{15}\text{N}$  *L*-histidine.H $_2\text{O}$ .HCl and C $\gamma_2(\text{V})$ -C $\beta(\text{L})$  in the dipeptide Ac-U- $^{13}\text{C}$ ,  $^{15}\text{N}$  *L*-valine-*L*-leucine (AcVL). In each case, two separate experiments were performed, namely a dipolar-modulated (full symbols) and a reference (open symbols) experiment. In the latter reference experiment, an equivalent double Gaussian pulse is used, but

its frequency is positioned such that only one of the two signals is selected, thus allowing the spin-echo dephasing time,  $T_2'$ , to be independently determined. In this work, the offset from the magic angle,  $\Delta$ , was determined using the sensitivity of the  $1-^{13}\text{C}$  *L*-alanine lineshape to the angle offset (see ESI), though a Hall effect angle sensor<sup>37</sup> could also be used.

An extension of the theory of spin-echo MAS modulation for a homonuclear spin pair under a  $J$  coupling<sup>38</sup> to the case of off MAS is presented in the SI (see eqns E7 & E9) of Ref.<sup>24</sup> Specifically, for the case where the through-bond  $J$  coupling is zero,  $s(\tau)$  for the dipolar-modulated experiment is given by (neglecting here the  $T_2^0$  term in Ref.<sup>24</sup>):

$$s(\tau) = A \exp(-\tau / T_2') (1/2) \times \int_0^\pi \cos\{\pi\sqrt{2}D\Delta(3\cos^2\beta - 1)(\tau - t_s)\} \sin\beta d\beta, \quad (1)$$

where the integral corresponds to a powder average over the angle,  $\beta$ , between the internuclear vector of the dipolar-coupled spins and the rotor axis. The calculation of the time shift,  $t_s$ , due to the finite length of the refocusing pulse is described in the ESI, using the procedure employed in Ref.<sup>25</sup> Note that the offset,  $\Delta$ , from the magic angle in eqn (1) is in radians, while the dipolar coupling constant,  $D$ , is in Hz:

$$D = \left( -\frac{\mu_0 \gamma^2 \hbar}{4\pi r^3} \right) / 2\pi, \quad (2)$$

where  $r$  is the internuclear distance and  $\gamma$  is the magnetogyric ratio of the nuclei (here  $^{13}\text{C}$ ).

As well as the use of the angle-switching probe, a novel feature of the experimental protocol described here is the use of the separate reference experiment (see open symbols in Fig. 2). The spin-echo intensities,  $s(\tau)$ , for the reference experiment are fitted to:

$$s(\tau) = A \exp(-\tau / T_2'), \quad (3)$$

thus allowing the independent determination of  $T_2'$ . Note that the so-determined  $T_2'$  for the off-angle spin-echo evolution includes the effect of dipolar modulation due to like spins, i.e., intermolecular  $^{13}\text{C}$ - $^{13}\text{C}$  (U- $^{13}\text{C}$ ,  $^{15}\text{N}$  *L*-histidine.H $_2\text{O}$ .HCl) and  $^{13}\text{C}\gamma_2(\text{V})$ - $^{13}\text{C}\gamma_2(\text{V})$  (AcVL) dipolar couplings for the experimental data in Fig. 2. The advantage of this procedure is that, for the dipolar-modulated  $s(\tau)$ , this leaves only  $D$  as a free variable for fitting. Best fits in Fig. 2a and 2b are shown as solid and dashed lines for the dipolar-modulated (fit to eqn (1)) and reference (fit to eqn (3)) data, respectively. Table 1 lists the fitted  $D$  (together with the corresponding internuclear distance,  $r$ ) and  $T_2'$  values as well as the offset from the magic angle,  $\Delta$ , and the time shift,  $t_s$ .

The packing together in the solid state of the uniformly  $^{13}\text{C}$  labelled molecules means that intermolecular as well as intramolecular dipolar couplings can contribute to the observed dipolar modulation. This is expressed via the root-

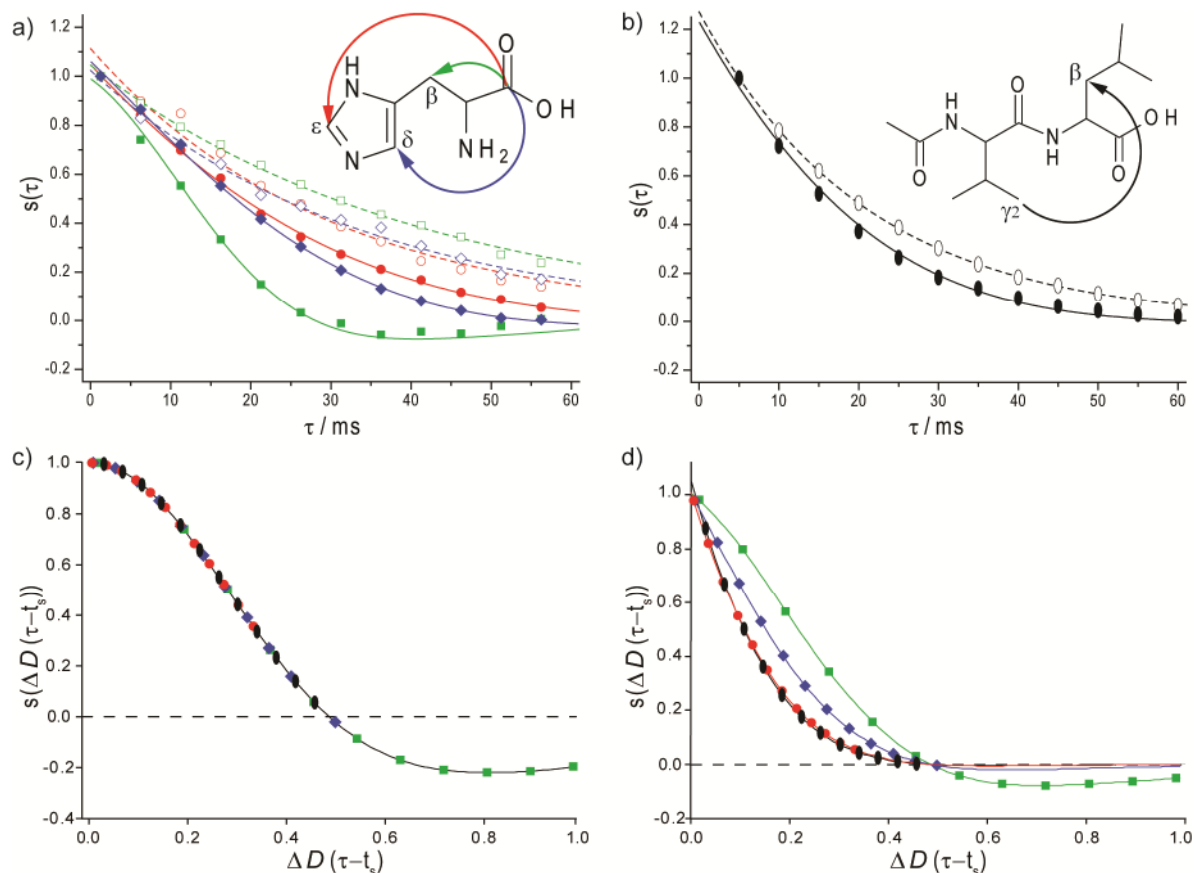


**Fig. 2** (a,b) Dipolar-modulated (full symbols) and reference (open symbols) spinning-angle-encoded  $^{13}\text{C}$  (150 MHz, 12 kHz MAS) NMR spin-echo ( $\tau/2 - \pi - \tau/2$ ) curves recorded using the pulse sequence in Fig. 1 for the (a) CO-C $\beta$  (green squares), CO-C $\delta$  (blue diamonds) and CO-C $\epsilon$  (red circles) pairs in U- $^{13}\text{C}$ ,  $^{15}\text{N}$ -histidine.H $_2$ O.HCl and (b) the C $_{\gamma_2}$ (V)-C $\beta$ (L) pair in Ac-U- $^{13}\text{C}$ ,  $^{15}\text{N}$ -Val-Leu. Best-fits to eqn (1) and eqn (3) are shown as solid and dashed lines, respectively (see Table 1). The signal intensity was integrated for the CO (His) or C $_{\gamma_2}$ (V) resonances (after Fourier transformation with respect to the acquisition time,  $t_2$ ), with the experimental noise being less than  $\pm 0.02$ . (c,d) The analytical expression for  $s(\tau)$  in eqn (1) defines a master curve that depends on  $\Delta$  (in radians),  $D$  (in Hz), and  $\tau - t_s$  (in s). Using the best-fit  $D$  values (see Table 1), the green squares, blue diamonds, red circles and black ellipsoids correspond to the  $\tau$  (and  $\Delta$  and  $t_s$ ) values for the experimental data in (a,b). The spin-echo dephasing term,  $\exp(-\tau/T_2')$  (see Table 1), is neglected in (c) and included in (d).

sum-squared dipolar coupling,  $D_{\text{rss}}$ ,<sup>39-40</sup> that takes into account all (intra- and intermolecular) C-C distances for the same pair of nuclei:

$$D_{\text{rss}} = \sqrt{\sum D_{ij}^2}. \quad (4)$$

The  $D_{\text{rss}}$  values determined from the corresponding single-crystal diffraction structures (CSD codes: HISTCM12 and JAYNUS)<sup>41-42</sup> are listed in Table 1. Note that while the shortest C-C distances for the CO-C $\beta$  (2.57 Å) and CO-C $\delta$  (3.11 Å) pairs in *L*-histidine.H $_2$ O.HCl are intramolecular, they are intermolecular for the CO-C $\beta$  (4.05 Å) pair in *L*-histidine.H $_2$ O.HCl and the C $_{\gamma_2}$ (V)-C $\beta$ (L) pair (5.26 Å) in AcVL. Thus, for the C $_{\gamma_2}$ (V)-C $\beta$ (L) pair in AcVL, the effective distance of 4.36 Å stated in Table 1 corresponds to a sum over multiple distances of 5.26 Å and longer.

A further novel feature of this work is the recognition that the analytical expression for  $s(\tau)$ , eqn (1), defines a master curve that depends on  $\Delta$ ,  $D$ , and  $\tau - t_s$ . This is illustrated by Fig. 2c and 2d for the best-fit  $D$  values, where the green squares, blue diamonds, red circles and black ellipsoids

**Table 1** Spinning-angle-encoded spin-echo fits

spin pair	$\Delta^a$	$t_s$ [ms] <sup>b</sup>	$T_2'$ [ms] <sup>c</sup>	fitted distance <sup>de</sup>	effective distance <sup>df</sup>
CO-C $\beta$ (His)	2.3°	0.3	41 ± 1	2.59 ± 0.02 Å (437 ± 9 Hz)	2.55 Å (460 Hz)
CO-C $\delta$ (His)	2.3°	0.3	33 ± 1	3.25 ± 0.03 Å (222 ± 6 Hz)	3.01 Å (278 Hz)
CO-C $\epsilon$ (His)	2.3°	0.3	30 ± 1	3.72 ± 0.06 Å (148 ± 7 Hz)	3.43 Å (252 Hz)
C $_{\gamma_2}$ (V)-C $\beta$ (L) (AcVL)	4.2°	1.2	21 ± 1	4.15 ± 0.06 Å (106 ± 6 Hz)	4.36 Å (92 Hz)

<sup>a</sup> Determined from the sensitivity of the 1- $^{13}\text{C}$  *L*-alanine lineshape to the angle offset (see ESI). Note that  $\Delta$  in this Table is specified in degrees, while  $\Delta$  is specified in radians in eqn (1) and the master curve representations in Fig. 2c and 2d. <sup>b</sup> Calculated as described in Ref.<sup>25</sup> (see ESI). <sup>c</sup> Determined from fitting the reference curve to eqn (3). <sup>d</sup> The corresponding dipolar coupling is given in brackets. <sup>e</sup> Determined from fitting the dipolar-modulated curve to eqn (1). <sup>f</sup>  $D_{\text{rss}}$  is given in eqn (4) (all atoms within 10 Å were considered for the corresponding crystal structures).

correspond to the  $\tau$  (and  $\Delta$  and  $t_s$ ) values for the experimental data in Fig. 2a and 2b. Specifically, the master-curve presentation in Fig. 2c shows how the probing of a smaller  $D$  for the > 4 Å effective distance in the dipeptide is enabled by

using a larger  $\Delta$  ( $4.2^\circ$  as compared to  $2.3^\circ$ ).

Fig. 2d shows the effect of the different experimental  $T_2'$  values (see Table 1); the spin-echo dephasing term is neglected in Fig. 2c. Ideally, the zero crossing should be observed, however spin-echo dephasing which is dependent on  $^1\text{H}$  decoupling performance<sup>43</sup> precludes this for all cases except the shorter CO-C $\beta$  distance (in this case, the determined NMR distance is within 2 % of the effective distance determined from  $D_{\text{rfs}}$  for the crystal structure). Nevertheless, the reference curve approach used here ensures good agreement (within 10 %) between the fitted distance and the effective distance determined from the  $D_{\text{rfs}}$  for the crystal structure, for the case of effective distances up to  $4.5 \text{ \AA}$ . In future work, multi-spin simulations will be used to better understand factors that could lead to such small discrepancies.

## Conclusions

In conclusion, using the simple spin-echo experiment in Fig. 1 and a fast angle switching probe, longer-range C-C distances can be accurately determined in uniformly  $^{13}\text{C}$  labeled samples, notably the greater than  $4 \text{ \AA}$  C $\gamma_2(\text{V})$ -C $\beta(\text{L})$  distance in the dipeptide Ac-VL. The new experimental protocol presented here involves the recording of separate dipolar-modulated and reference spin-echo datasets that correspond to changing the irradiation frequencies of the double Gaussian pulse: this enables the independent determination of the spin-echo dephasing time,  $T_2'$ , such that the dipolar coupling is the only free variable for the fit of the dipolar-modulated data. This method can be extended to larger molecules and other nuclei (e.g.,  $^1\text{H}$ ), with the only requirement being the necessity to selectively excite the specific pair of resonances by the cosine-modulated Gaussian pulse, with the further possibility of incorporating off-MAS spin-echo modulation into a higher-dimensional experiment. The master curve presentation in Fig. 2c shows that larger angle offsets would enable the more accurate measurement of longer distances, thus motivating further development of switched-angle probe technology.

## Acknowledgements

Funding from EPSRC is acknowledged. We thank M.H. Levitt and G. Pileio for helpful discussions.

## Notes and references

<sup>a</sup> Department of Physics, University of Warwick, Coventry, UK CV4 7AL. Fax: +44 24 76150897; Tel: +44 24 76574359; E-mail: s.p.brown@warwick.ac.uk

<sup>b</sup> Present address: Institute of Biophysical Chemistry, Johann Wolfgang Goethe-University Frankfurt, Max-von-Laue-Straße 9, 60438 Frankfurt am Main, Germany.

<sup>c</sup> MAS Systems and Tallinn University of Technology, Ehitajate 5, Tallinn, Estonia. E-mail: ago.samoson@gmail.com

† Electronic Supplementary Information (ESI) available: [Further details: angle switching; angle calibration; the double Gaussian selective pulses]. See DOI: 10.1039/b000000x/

1. A. McDermott, *Ann. Rev. Biophys.*, 2009, **38**, 385.
2. A. Lesage, *Phys. Chem. Chem. Phys.*, 2009, **11**, 6876.

3. S. O. Smith, D. Song, S. Shekar, M. Groesbeek, M. Ziliox and S. Aimoto, *Biochemistry*, 2001, **40**, 6553.
4. F. Castellani, B. van Rossum, A. Diehl, M. Schubert, K. Rehbein and H. Oschkinat, *Nature*, 2002, **420**, 98.
5. C. Wasmer, A. Lange, H. Van Melckebeke, A. B. Siemer, R. Riek and B. H. Meier, *Science*, 2008, **319**, 1523.
6. W. T. Franks, B. J. Wylie, H. L. F. Schmidt, A. J. Nieuwkoop, R. M. Mayrhofer, G. J. Shah, D. T. Graesser and C. M. Rienstra, *Proc. Natl. Acad. Sci. U. S. A.*, 2008, **105**, 4621.
7. I. Bertini, L. Emsley, M. Lelli, C. Luchinat, J. F. Mao and G. Pintacuda, *J. Am. Chem. Soc.*, 2010, **132**, 5558.
8. M. Carravetta, M. Eden, O. G. Johannessen, H. Luthman, P. J. E. Verdegem, J. Lugtenburg, A. Sebald and M. H. Levitt, *J. Am. Chem. Soc.*, 2001, **123**, 10628.
9. P. Hodgkinson and L. Emsley, *J. Magn. Reson.*, 1999, **139**, 46.
10. M. Hohwy, C. M. Rienstra and R. G. Griffin, *J. Chem. Phys.*, 2002, **117**, 4973.
11. M. J. Bayro, M. Huber, R. Ramachandran, T. C. Davenport, B. H. Meier, M. Ernst and R. G. Griffin, *J. Chem. Phys.*, 2009, **130**, 114506.
12. V. Ladizhansky, *Solid State Nucl. Magn. Reson.*, 2009, **36**, 119.
13. I. Marin-Montesinos, G. Mollica, M. Carravetta, A. Gansmuller, G. Pileio, M. Bechmann, A. Sebald and M. H. Levitt, *Chem. Phys. Lett.*, 2006, **432**, 572.
14. A. K. Paravastu and R. Tycko, *J. Chem. Phys.*, 2006, **124**, 194303.
15. R. Tycko, *Phys. Rev. Lett.*, 2007, **99**, 187601.
16. N. Khaneja and N. C. Nielsen, *J. Chem. Phys.*, 2008, **128**, 015103.
17. L. A. Straaso, M. Bjerring, N. Khaneja and N. C. Nielsen, *J. Chem. Phys.*, 2009, **130**, 225103.
18. J. Spano and S. Wi, *J. Magn. Reson.*, 2010, **204**, 314.
19. P. T. F. Williamson, A. Verhoeven, M. Ernst and B. H. Meier, *J. Am. Chem. Soc.*, 2003, **125**, 2718.
20. A. Verhoeven, P. T. F. Williamson, H. Zimmermann, M. Ernst and B. H. Meier, *J. Magn. Reson.*, 2004, **168**, 314.
21. K. Nomura, K. Takegoshi, T. Terao, K. Uchida and M. Kainosho, *J. Am. Chem. Soc.*, 1999, **121**, 4064.
22. R. Ramachandran, V. Ladizhansky, V. S. Bajaj and R. G. Griffin, *J. Am. Chem. Soc.*, 2003, **125**, 15623.
23. X. H. Peng, D. Libich, R. Janik, G. Harauz and V. Ladizhansky, *J. Am. Chem. Soc.*, 2008, **130**, 359.
24. G. Pileio, Y. Guo, T. N. Pham, J. M. Griffin, M. H. Levitt and S. P. Brown, *J. Am. Chem. Soc.*, 2007, **129**, 10972.
25. G. Pileio, S. Mamone, G. Mollica, I. M. Montesinos, A. Gansmuller, M. Carravetta, S. P. Brown and M. H. Levitt, *Chem. Phys. Lett.*, 2008, **456**, 116.
26. C. P. Jaronec, B. A. Tounge, J. Herzfeld and R. G. Griffin, *J. Am. Chem. Soc.*, 2001, **123**, 3507.
27. J. Trebosc, J. P. Amoureux, L. Delevoye, J. W. Wiench and M. Pruski, *Solid State Sci.*, 2004, **6**, 1089.
28. S. Cadars, A. Lesage, N. Hedin, B. F. Chmelka and L. Emsley, *J. Phys. Chem. B*, 2006, **110**, 16982.
29. P. L. Stewart, R. Tycko and S. J. Opella, *J. Chem. Soc., Faraday Trans.*, 1988, **84**, 3803.
30. B. M. Fung, A. M. Khitrin and K. Ermolaev, *J. Magn. Reson.*, 2000, **142**, 97.

- 
31. G. Metz, X. L. Wu and S. O. Smith, *J. Magn. Reson. Ser. A*, 1994, **110**, 219.
32. S. Hediger, B. H. Meier, N. D. Kurur, G. Bodenhausen and R. R. Ernst, *Chem. Phys. Lett.*, 1994, **223**, 283.
- 5 33. S. P. Brown, M. Perez-Torralba, D. Sanz, R. M. Claramunt and L. Emsley, *Chem. Commun.*, 2002, 1852.
34. S. P. Brown and L. Emsley, *J. Magn. Reson.*, 2004, **171**, 43.
35. T. N. Pham, J. M. Griffin, S. Masiero, S. Lena, G. Gottarelli, P. Hodgkinson, C. Filip and S. P. Brown, *Phys. Chem. Chem. Phys.*,  
10 2007, **9**, 3416.
36. I. Hung, A. C. Uldry, J. Becker-Baldus, A. L. Webber, A. Wong, M. E. Smith, S. A. Joyce, J. R. Yates, C. J. Pickard, R. Dupree and S. P. Brown, *J. Am. Chem. Soc.*, 2009, **131**, 1820.
37. S. Mamone, A. Dorsch, O. G. Johannessen, M. V. Naik, P. K. Madhu  
15 and M. H. Levitt, *J. Magn. Reson.*, 2008, **190**, 135.
38. L. Duma, W. C. Lai, M. Carravetta, L. Emsley, S. P. Brown and M. H. Levitt, *ChemPhysChem*, 2004, **5**, 815.
39. V. E. Zorin, S. P. Brown and P. Hodgkinson, *Mol. Phys.*, 2006, **104**, 293.
- 20 40. V. E. Zorin, S. P. Brown and P. Hodgkinson, *J. Chem. Phys.*, 2006, **125**, 144508.
41. J. Donohue and A. Caron, *Acta Crystallogr.*, 1964, **17**, 1178.
42. P. J. Carroll, P. L. Stewart and S. J. Opella, *Acta Crystallogr. C*, 1990, **46**, 243.
- 25 43. G. De Paepe, N. Giraud, A. Lesage, P. Hodgkinson, A. Bockmann and L. Emsley, *J. Am. Chem. Soc.*, 2003, **125**, 13938.